Scaling-Up ^{129}Xe Hyperpolarization - Theoretical Modeling

I. C. Ruset[1,2], F. W. Hersman[1,2], R. Carrier[3], S. D. Covrig[1], A. Sindile[1], and J. Distelbrink[2]

[1]Department of Physics, University of New Hampshire, Durham, NH, United States, [2]XEMED, Durham, NH, United States, [3]Research Computing Center, University of New Hampshire, Durham, NH, United States

Introduction

Hyperpolarized gas MRI has been demonstrated more than a decade ago [1]. Although ^{129}Xe was the first hyperpolarized gas to be used in this type of application, the research community has focused on ^{3}He studies, mainly because of the larger quantities of hyperpolarized gas available. Xenon has many advantages over helium, such as natural abundance, lower diffusion, and large partition coefficient in blood. It can be used as a tracer and presents a frequency chemical shift when dissolved in blood, tissue, brain, or trapped in molecular cages [2]. The hold-back in Xe applications has been mainly the hyperpolarizing methods and the limited quantities of polarized gas available. A new design of a high-flow low-pressure SEOP (spin-exchange optical pumping) Rb-Xe polarizer was recently demonstrated [3]. The concept of counterflowing the gas mixture against laser light and dividing the polarizing cell in three operational zones has resulted in an increase with over an order of magnitude in the output magnetization compared with previously reported polarizers. Nonetheless, detailed experimental studies have shown saturation of the output polarization with the laser power after a certain limit. This is shown in Fig.1. Turbulent convective flow was also visible after increasing the local laser absorption through a higher Rb depolarization rate (higher Xe concentration). Consequentially, we modeled the polarizer in a 2D axial-symmetrical geometry as a first step in overcoming these limitations in future polarizer designs. The theoretical model, preliminary results, and future optimization plans of the Xe polarizer will be discussed.

Methods

The progress of diode laser technology with kilowatt output power and novel optical systems development [5] can redefine the limits of hyperpolarizing noble gases technology if the side-effects, such as heating of the gas mixture after laser absorption, would be minimized [4]. Previous polarizing system suffered from a strong coupling of the optical pumping parameters, such as Rb vapor density runaways because of laser heating effects [8]. Using a novel polarizer design to separate the hyperpolarizing steps in separate chambers we surpassed most of these correlations. In the demonstrated design the polarizing column is separated in three regions: Rb saturator, optical pumping region, and Rb condensing region [3]. The total pressure of the gas mixture is chosen such that the spin-exchange is dominated by the more efficient Rb-Xe van der Waals molecular interaction [6].

For the modeling we used a cylindrical geometry 4 cm diameter and 1.8 meter long separated into a hot SEOP region (1.0 m) and a Rb condensing cold region (0.8 m). We assume that the gas mixture enters the SEOP region pre-saturated with Rb vapor. Because of the relative low flow rate (~1.5 liters/minute) we considered a gas mixture laminar flow established within the column over which we superposed the advection-diffusion equation for Rb density. Due to the fast optical pumping process of Rb (~ms) its polarization is considered at steady-state. Xenon polarization builds-up as the gas mixture travels through the column against the laser light. Xenon is exposed to the highest Rb polarization before exiting the optical pumping region. Finally, the output Xe polarization is averaged over the laminar flow at the exit from the column. The laser power loss is accounted for and is assumed to be completely dissipated as heat inside the gas mixture. The heat equation is included to calculate the gas mixture temperature. Since the total pressure is controlled at a constant value, local gas mixture and Rb vapor density depends on the temperature. Although very little is known, the spin-exchange and spin-destruction rates have also temperature dependence included. This is probably the major source of error in the model. In an ongoing project our group plans to study in detail the temperature dependencies of Rb-Xe optical pumping parameters. For now, we consider the binary velocity-averaged cross sections to have $T^{0.5}$ dependence, while the van der Waals molecular rates have $T^{-2.5}$ dependence [7].

Results

The current version of the code is capable of outputting 2D maps of the polarizations, temperature, Rb density, etc. Two examples are shown in Fig.2 and 3. Fig.2 shows Rb polarization near the wall surface confirming that Rb polarization dead-layer is insignificant to the SEOP process. This was observed for all laser powers and xenon concentrations used in our simulations. Fig.3 shows one example of xenon polarization build-up as it travels through the polarizer. Maximum polarization is achieved towards the edge where gas mixture velocity is smaller and Xe has a longer interaction time with polarized Rb. However, within millimeters from to the wall surface Xe polarization decreases because of low Rb polarization numbers. We are presently seeking methods to predict and overcome polarization limitations. At this stage the program is not confirming the polarization saturation at only 70W of narrowed-spectrum laser power observed experimentally and shown in Fig.1. The code shows polarization saturation at much higher values of laser power. It predicts a faster Xe polarization saturation in the case of the narrowed-spectrum laser at ~400W compared with broad laser at ~750 W. The disagreement can be caused by the low level of knowledge of the Rb-Xe spin-exchange rates and their temperature dependence. Future versions of the program will have implemented optimization routines for finding the optimum geometry and operating parameters in order to maximize Xe polarization, magnetization, or other user-defined variables. Heat convection and radiation trapping effects on Rb polarization will be included as well. We expect a much better agreement with the experimental results by updating the spin-exchange and spin-destruction cross-section constants after precise measurements in our diagnostics system (presented elsewhere). A web interface of the program is accessible on-line at http://xenon.unh.edu.

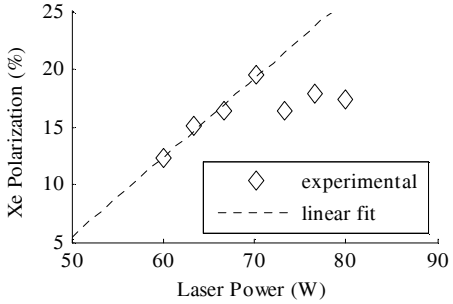

Fig.1: Xenon polarization as a function of the laser power saturates at unexpected low power values. The laser is a 0.5nm FWHM narrowed-spectrum laser. This dependence was not observed for a typical 1.5nm FWHM diode laser.

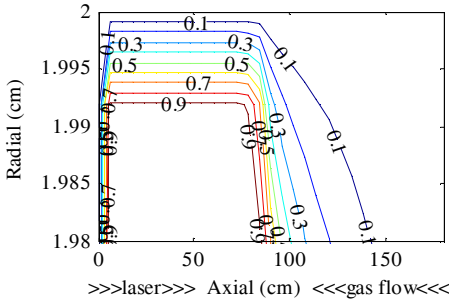

Fig.2 Rb polarization in the vicinity of the glass surface (2mm) shows a micron size "dead"-layer. The model considers full relaxation of Rb on the wall surface, however this result shows that Rb wall relaxation is negligible compared with Rb-Xe relaxation.

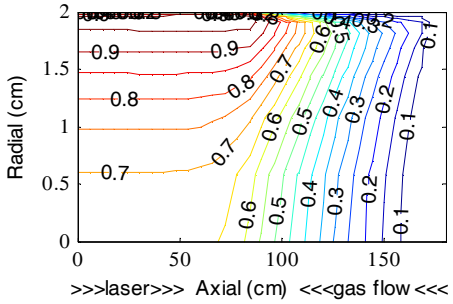

Fig.3 Xenon polarization contour map showing polarization build-up as the gas mixture travels from right to left against the laser light and through polarized Rb vapor. Conditions: 10 sccm Xe, 350 sccm N2, 990 sccm He, 500 torr, 160°C SEOP region, 27°C cold region, 100 W laser power (1.5nm).

References:

[1] M.S. Albert et al. *Nature (London)* **370**: 199 (1994).
[2] B.M. Goodson *J. Magn. Reson.* **155**: 157 (2002).
[3] I.C. Ruset, S. Ketel, F.W. Hersman *Phys. Rev. Lett.* **96**: 053002 (2006).
[4] D.K. Walter, W.M. Griffith, W. Happer *Phys. Rev. Lett.* **86**: 3264 (2001).
[5] H. Zhu, I.C. Ruset, F.W. Hersman *Opt. Lett.* **30**: 1342 (2005).
[6] W. Happer et al. *Phys. Rev. A* **29**: 3092 (1984).
[7] I.A. Nelson, T.G. Walker *Phys. Rev. A* **29**: 0127121 (2001).
[8] A.L. Zook, B.B. Adhyaru, C.R. Bowers *J. Magn. Reson.* **159**: 175 (2002).